Applied Mathematics & Information Sciences **4**(3) (2010), 413–428
– An International Journal
©2010 Dixie W Publishing Corporation, U. S. A.

Deformation Due to Inclined Load in an Orthotropic Micropolar Thermoelastic Medium with Two Relaxation Times

Rajneesh Kumar[1] and Rajani Rani Gupta[2]

Department of Mathematics, Kurukshetra University, Kurukshetra-136 119, India
[1]*Email Address: rajneesh_kuk@rediffmail.com*
[2]*Email Address: rajani_gupta_83@yahoomail.com*

Received January 3, 2009; Revised May 1, 2009

The present investigation is concerned with deformation in an orthotropic micropolar thermoelastic solid with two relaxation times as a result of inclined load. The inclined load is assumed to be linear combination of a normal load and a tangential load. Integral transform technique is used to solve the problem. Expressions of stresses and temperature distribution are obtained in physical domain, by using a numerical inversion technique. Various type of forces have been taken to illustrate the utility of the approach. The expressions for frequency domain and steady state are also obtained with appropriate change of variables. Stresses and temperature distribution are shown graphically to evince the response of different forces and effect of change in angle of inclination.

Keywords: Orthotropic micropolar thermoelastic solid, couple stress, integral transform, microrotation.

1 Introduction

A micropolar elastic solid is an elastic solid whose deformation can be described by a 'macro' displacement together with a 'micro' rotation. Micropolar elastic materials are the elastic materials with extra independent degree of freedom for local rotations. They include certain class of materials with fibrous and elongated grains. The theory of micropolar elasticity introduced and developed by Eringen [1–3] has aroused much interest in recent years, because of its possible utility in investigating deformation properties of solids for which the classical theory is inadequate. This theory is believed to be particularly useful in investigating materials consisting of bar like molecules which exhibit microrotational effects and which can support body and surface couples. Furthermore, the micropolar

elastic model is considered to be more realistic than the classical elastic model in studying earth science problems [4].

The linear theory of micropolar thermoelasticity was developed by extending the theory of micropolar continua to include thermal effects by Nowacki [5] and Eringen [6]. Tauchert *et al.* [7] also derived the basic equations of linear theory of micropolar thermoelasticity. Dost and Tabarrok [8] presented the micropolar generalised thermoelasticity by using Green -Lindsay theory. One can refer to Dhaliwal and Singh [9] for a review on the micropolar thermoelasticity. Chandrasekhariah [10] formulated a theory of micropolar thermoelasticity which includes heat-flux among the constitutive variables.

The dynamic response functions of elastically anisotropic solids are of interest in many fields including crystal acoustics, solid-state physics, nondestructive testing, material characterisation, seismology, applied mathematics and mechanics. In recent years, the elastodynamic response of anisotropic continuum has received the attention of several researches.

Iesan [11] studied the static theory of anisotropic micropolar elastic solids and proved the positive definiteness of his operator for the first boundary value problem. Kumar *et al.* [12–19] discussed various problems in inclined load and orthotropic micropolar continua.

The present investigation seeks to determine the components of normal stress, tangential couple stress and temperature distribution due to concentrated, distributed and moving forces in time domain, frequency domain and steady state due to inclined load in micropolar orthotropic generalized thermoelastic medium. The solution is obtained after employing an integral transform technique, which is inverted by using a numerical method.

2 Formulation and Solution of the Problem

We consider an orthotropic micropolar generalized thermoelastic half-space, with x_2-axis pointing vertically into the medium. Suppose that an inclined load F_0, per unit length is acting along the interface on the x_3-axis and its inclination with x_2-axis is θ.

The basic equations in dynamic theory of the plain strain of a homogeneous, orthotropic micropolar thermoelastic solid with two relaxation times in absence of body forces, body couples and heat sources are

$$t_{ji,j} = \rho \ddot{u}_i, \tag{2.1}$$

$$m_{ik,i} + \varepsilon_{ijk} t_{ij} = \rho j \ddot{\phi}_k,\ i,j,k = 1,2,3, \tag{2.2}$$

and heat conduction equation is

$$K_1^* \frac{\partial^2 T}{\partial x_1^2} + K_2^* \frac{\partial^2 T}{\partial x_2^2} = \Big(\frac{\partial T}{\partial t} + \tau_0 \frac{\partial^2 T}{\partial t^2}\Big)\Big(\rho C^* + \beta_1 T_0 \frac{\partial u_1}{\partial x_1} + \beta_2 T_0 \frac{\partial u_2}{\partial x_2}\Big). \tag{2.3}$$

The constitutive relations are

$$t_{11} = A_{11}\varepsilon_{11} + A_{12}\varepsilon_{22} - \beta_1(1 + \tau_1 \frac{\partial}{\partial t})T, \qquad t_{12} = A_{77}\varepsilon_{12} + A_{78}\varepsilon_{21},$$

$$t_{22} = A_{12}\varepsilon_{11} + A_{22}\varepsilon_{22} - \beta_2(1 + \tau_1\frac{\partial}{\partial t})T, \qquad t_{21} = A_{78}\varepsilon_{12} + A_{88}\varepsilon_{21},$$
$$m_{13} = B_{66}\phi_{3,1}, \qquad m_{23} = B_{44}\phi_{3,2}, \tag{2.4}$$

where

$$\varepsilon_{ij} = u_{j,i} + \epsilon_{ji3}\phi_3. \tag{2.5}$$

Here the relations between β_i and the coefficients of thermal expansions α_i, $i = 1, 2$, are

$$\beta_1 = A_{11}\alpha_1 + A_{12}\alpha_2, \qquad \beta_2 = A_{21}\alpha_1 + A_{22}\alpha_2,$$

where α_1 are the coefficients of linear thermal expansion.

In these relations, t_{ij} are components of the stress tensor, m_{ij} are components of the couple stress, ε_{ij} are components of micropolar strain tensor, u_i are components of displacement vector, ϕ_3 is the component of microrotation vector, ϵ_{ijk} is the permutation symbol, τ_0, τ_1 are the relaxation times, C^* is the specific heat at constant strain, K_1^* and K_2^* are the thermal conductivities, A_{11}, A_{12}, A_{22}, A_{77}, A_{78}, A_{88}, B_{44}, and B_{66} are characteristic constants of the material.

For the two dimensional problem, we assume the components of the displacement and microrotation vector for orthotropic micropolar generalized thermoelastic solid be of the form

$$\vec{u} = (u_1, u_2, 0), \quad \vec{\phi} = (0, 0, \phi_3). \tag{2.6}$$

We define the nondimensional variables by the expressions:

$$x_1' = \frac{\omega^* x_1}{c_1},\ x_2' = \frac{\omega^* x_2}{c_1},\ u_1' = \frac{\rho c_1\omega^* u_1}{\beta_1 T_0},\ u_2' = \frac{\rho c_1\omega^* u_2}{\beta_1 T_0},\ \phi_3' = \frac{\rho c_1^2}{\beta_1 T_0}\phi_3,\ t_{ij}' = \frac{t_{ij}}{\beta_1 T_0},$$
$$m_{23}' = \frac{\omega^*}{c_1\beta_1 T_0}m_{23},\ T' = \frac{T}{T_0},\ t' = \omega^* t,\ \tau_0' = \omega^*\tau_0,\ \omega' = \frac{\omega}{\omega^*}, \tag{2.7}$$

where

$$\omega^* = \frac{\rho C^* c_1^2}{K_1^*}, \quad c_1^2 = \frac{A_{11}}{\rho}.$$

With the help of equations (2.4)-(2.7), equations (2.1)-(2.3) take the form (on suppressing the prime)

$$\Big(\frac{\partial^2}{\partial x_2^2} + d_1 d_4\frac{\partial^2}{\partial x_1^2}\Big)u_1 + (d_2 + d_3)\frac{\partial^2 u_2}{\partial x_1\partial x_2} - (d_3 - 1)\frac{\partial\phi_3}{\partial x_2} - d_1 d_4\frac{\partial}{\partial x_1}\Big(1 + \tau_1\frac{\partial}{\partial t}\Big)T = d_1 d_4\frac{\partial^2 u_1}{\partial t^2}, \tag{2.8}$$

$$\frac{d_2 + d_3}{d_4}\frac{\partial^2 u_1}{\partial x_1\partial x_2} + \Big(\frac{\partial^2}{\partial x_2^2} + \frac{d_5}{d_4}\frac{\partial^2}{\partial x_1^2}\Big)u_2 - \frac{d_5 - d_3}{d_4}\frac{\partial\phi_3}{\partial x_1} - \bar{\beta} d_1\frac{\partial}{\partial x_2}\Big(1 + \tau_1\frac{\partial}{\partial t}\Big)T = d_1\frac{\partial^2 u_2}{\partial t^2}, \tag{2.9}$$

$$\Big(\frac{\partial^2}{\partial x_2^2} + d_6\frac{\partial^2}{\partial x_1^2} - d_7(d_5 - 2d_3 + 1)\Big)\phi_3 + d_7(d_3 - 1)\frac{\partial u_1}{\partial x_2} + d_7(d_5 - d_3)\frac{\partial u_2}{\partial x_1} = d_8\frac{\partial^2\phi_3}{\partial t^2}, \tag{2.10}$$

$$\Big(\frac{\partial^2}{\partial x_1^2}+\bar{K}\frac{\partial^2}{\partial x_2^2}\Big)T=\Big(\frac{\partial}{\partial t}+\tau_0\frac{\partial^2}{\partial t^2}\Big)T+\epsilon\Big(\frac{\partial}{\partial t}+\tau_0\frac{\partial^2}{\partial t^2}\Big)\Big(\frac{\partial u_1}{\partial x_1}+\bar{\beta}\frac{\partial u_2}{\partial x_2}\Big), \tag{2.11}$$

where

$$d_1=\frac{A_{11}}{A_{22}},\ d_2=\frac{A_{12}}{A_{88}},\ d_3=\frac{A_{78}}{A_{88}},\ d_4=\frac{A_{22}}{A_{88}},\ d_5=\frac{A_{77}}{A_{88}},\ \bar{K}=\frac{K_2^*}{K_1^*},$$

$$d_6=\frac{B_{66}}{B_{44}},\ d_7=\frac{A_{88}c_1^2}{B_{44}\omega^{*2}},\ d_8=\frac{\rho j c_1^2}{B_{44}},\ \bar{\beta}=\frac{\beta_2}{\beta_1},\ \epsilon=\frac{\beta_1^2T_0}{\rho K_1^*\omega^*}.$$

We define Laplace and Fourier Transform as

$$\bar{f}(x_1,x_2,p)=\int_0^\infty f(x_1,x_2,t)e^{-pt}dt, \tag{2.12}$$

and

$$\tilde{f}(\xi,x_2,p)=\int_{-\infty}^\infty \bar{f}(x_1,x_2,p)e^{\iota\xi x_1}dx_1, \tag{2.13}$$

under the support of initial conditions

$$u_1(x_1,x_2,0)=\frac{\partial u_1}{\partial t}|_{t=0}=0,\quad u_2(x_1,x_2,0)=\frac{\partial u_2}{\partial t}|_{t=0}=0,$$

$$\phi_3(x_1,x_2,0)=\frac{\partial \phi_3}{\partial t}|_{t=0}=0,\quad T(x_1,x_2,0)=\frac{\partial T}{\partial t}|_{t=0}=0.$$

It is also assumed that u_1,u_2,ϕ_3,T and their first order partial derivatives with respect to x_1 tend to zero as $x_2\longrightarrow\pm\infty$.

2.1 Boundary conditions

The boundary conditions on the surface $x_2=0$ are given by

$$t_{22}=-P_1\psi(x_1,t),\quad t_{21}=-P_2\psi(x_1,t),\quad m_{23}=0,\quad T=0, \tag{2.14}$$

where P_1 and P_2 are the magnitudes of force and $\psi(x_1,t)$ is the known functions defined below in the manuscript.

Applications

In all the following cases, we take $\eta(t)=H(t)$, whose Laplace transform with respect to t is

$$\tilde{\eta}(p)=\frac{1}{p}. \tag{2.15}$$

Concentrated Force: In the case of concentrated force, we take

$$\psi(x_1,t)=\Psi(x_1)\eta(t), \tag{2.16}$$

where $\Psi(x_1) = \delta(x_1)$ is the Dirac delta function. Applying (2.12) and (2.13) in equation (2.15), we get

$$\tilde{\psi}(\xi, p) = \tilde{\eta}(p). \tag{2.17}$$

Distributed Force: The solution due to force distributed over a strip load of nondimensional width $2a$, applied at the boundary $x_2 = 0$, is obtained by setting

$$\Psi(x_1) = H(x_1 + a) - H(x_1 - a). \tag{2.18}$$

In this case, we have

$$\tilde{\psi}(\xi, p) = \frac{2\sin(\xi a)}{\xi}\tilde{\eta}(p). \tag{2.19}$$

Moving Force: In the case of an impulsive force moving along the x_1-axis with uniform nondimensional speed V at $x_2 = 0$, we set

$$\psi(x_1, t) = \delta(x_1 - Vt)\eta(t), \tag{2.20}$$

in equation (2.16). Applying (2.13) in equation (2.20) and considering the value of $\tilde{\eta}(p)$ from (2.15), we can obtain

$$\tilde{\psi}(\xi, p) = \frac{1}{(p - i\xi V)}. \tag{2.21}$$

2.2 Time domain solution

Applying the Laplace and Fourier transform defined by equations (2.12) and (2.13) in equations (2.8)-(2.11), we obtain

$$\Big(\frac{d^2}{dx_2^2} - (\xi^2 + p^2)d_1d_4\Big)\tilde{u}_1 - i\xi(d_2 + d_3)\frac{d\tilde{u}_2}{dx_2} - (d_3 - 1)\frac{d\tilde{\phi}_3}{dx_2} + i\xi d_1d_4(1 + \tau_1 p)\tilde{T} = 0, \tag{2.22}$$

$$\frac{-i\xi(d_2+d_3)}{d_4}\frac{d\tilde{u}_1}{dx_2} + \Big(\frac{d^2}{dx_2^2} - \frac{\xi^2 d_5}{d_4} - d_1p^2\Big)\tilde{u}_2 + \frac{i\xi(d_5 - d_3)}{d_4}\tilde{\phi}_3 - \bar{\beta}(1 + \tau_1 p)d_1\frac{d\tilde{T}}{dx_2} = 0, \tag{2.23}$$

$$\Big(\frac{d^2}{dx_2^2} - \xi^2 d_6 - d_7(d_5 - 2d_3 + 1) - d_8p^2\Big)\tilde{\phi}_3 + d_7(d_3 - 1)\frac{d\tilde{u}_1}{dx_2} - d_7i\xi(d_5 - d_3)\tilde{u}_2 = 0, \tag{2.24}$$

$$\Big(\frac{d^2}{dx_2^2} - \frac{\xi^2 + p + \tau_0p^2}{\bar{K}}\Big)\tilde{T} - \frac{i\xi\epsilon(p + \tau_0p^2)}{\bar{K}}\tilde{u_1} - \frac{\epsilon\bar{\beta}(p + \tau_0p^2)}{\bar{K}}\frac{d\tilde{u}_2}{dx_2} = 0. \tag{2.25}$$

The system of equations (2.22)-(2.25) has a nontrivial solution if the determinant of coefficient of (u_1, u_2, ϕ_3, T) vanishes. After solving these equation we obtain a bi-quadratic

equation of the form

$$\Big(\frac{d^8}{dx_2^8}+A\frac{d^6}{dx_2^6}+B\frac{d^4}{dx_2^4}+C\frac{d^2}{dx_2^2}+D\Big)(\tilde{u}_1,\tilde{u}_2,\tilde{\phi}_3,\tilde{T})=0, \tag{2.26}$$

where

$$\begin{aligned}
A &= -f-a-a_{11}+\bar{\beta}^2 g-h+b+d_7e^2,\\
B &= f[a+a_{11}+h-b-d_7e^2]+g[-\bar{\beta}^2a-h\bar{\beta}^2-\epsilon\xi^2(2d_2+d_3+d_4)\bar{\beta}-\bar{\beta}^2d_7\epsilon e^2\\
&\quad+\xi^2\epsilon d_4]+a(a_{11}+h-b)-a'+p^2hd_1-\frac{\xi^2(d_3-d_4)(d_5-d_3)ed_7}{d_4}-a_{11}e^2d_7,\\
C &= f\{a_{11}d_7e^2+a[-a_{11}-h+2b-2hd_1p^2-\xi^2(2d_2+d_3+d_4)]\}\\
&\quad+g\{ah\bar{\beta}^2+\xi^2(d_4-d_3)\epsilon\bar{\beta}a-2\bar{\beta}\xi^2d_7\epsilon(d_5-d_3)e+\xi^2\epsilon d_4a_{11}\}+(a+h)a',\\
D &= (fh-\xi^2gd_4\epsilon)(a_{11}a+a'),\\
a &= \xi^2d_6+d_7(d_5-2d_3+1)+d_8p^2, \qquad b=\xi^2\frac{(d_2+d_3)(d_2+d_4)}{d_4},\\
e &= (d_3-1), \qquad f=\frac{\xi^2+p+\tau_0p^2}{\bar{K}}, \qquad g=(1+\tau_1p)\frac{p+\tau_0p^2}{\bar{K}}\,d_1,\\
h &= (\xi^2+p^2)d_1d_4, \qquad a_{11}=d_1p^2+\frac{\xi^2d_5}{d_4}, \qquad a'=\frac{\xi^2d_7(d_5-d_3)^2}{d_4}.
\end{aligned}$$

The solution of equation (2.26) satisfying the radiation condition that $\tilde{u}_1,\tilde{u}_2,\tilde{\phi}_3,\tilde{T}\to 0$ as $x_2\to\infty$ is

$$(\tilde{u}_1,\tilde{u}_2,\tilde{\phi}_3,\tilde{T})=\sum_{i=1}^{4}A_i(1,r_i,s_i,t_i)\mathrm{e}^{-q_ix_2}, \tag{2.27}$$

where

$$r_i=\frac{a_1q_i^5+a_2q_i^3+a_3q_i}{a_4q_i^4+a_5q_i^2+a_6}, \quad s_i=\frac{-a_1q_i^3+a_9q_i+r_i(a_{10}q_i^2-a_{11}}{a_7q_i^2-a_8},$$

$$t_i=\frac{-(q_i^2-h-i\xi q_ir_i(d_2+d_3)+i\xi s_iq_i(d_3-1)}{i\xi d_1d_4}, \quad a_1=\frac{\bar{\beta}}{i\xi d_4},$$

$$a_2=\frac{-\bar{\beta}h+\xi^2(d_2+d_3)-a\bar{\beta}+d_7e^2}{i\xi d_4}, \quad a_3=a\frac{\bar{\beta}h-\xi^2(d_2+d_3)-\xi^2d_7e(d_5-d_3)}{d_4i\xi},$$

$$a_4=1-\frac{\bar{\beta}(d_2+d_3)}{d_4}, \quad a_5=-a_{11}-a_4a-\frac{\bar{\beta}e(d_5-d_3)d_7}{d_4}, \quad a_6=aa_{11}-a',$$

$$a_7=\frac{\bar{\beta}e}{i\xi d_4}, \quad a_8=\frac{i\xi(d_5-d_3)}{d_4}, \quad a_9=\frac{\bar{\beta}h-\xi^2(d_2+d_3)}{i\xi d_4}, \quad a_{10}=1-\frac{\bar{\beta}(d_2+d_3)}{d_4}.$$

Using equations (2.4), (2.6), and (2.7) in the boundary conditions (2.14) and then applying Laplace and Fourier transforms defined by equations (2.12) and (2.13) together with

the help of (2.27), we obtain the transformed normal stress, tangential stress, tangential couple stress and temperature distribution as

$$(\tilde{t}_{21}, \tilde{m}_{23}, \tilde{t}_{22}, \tilde{T}) = \frac{1}{\Delta}\sum_{k=1}^{4} \Delta_k(a_k^*, b_k^*, c_k^*, t_k)\mathrm{e}^{-q_k x_2}, \tag{2.28}$$

where

$$\begin{aligned}
a_k^* &= \frac{-d_3 i\xi r_k - q_k - e s_k}{d_1 d_4}, \quad b_k^* = -\frac{q_k s_k}{d_1 d_4 d_7}, \quad c_k^* = \frac{-d_2 i\xi - q_k r_k d_4 - \bar{\beta} t_k d_1 d_4}{d_1 d_4},\\
\Delta &= (c_1^* a_2^* - c_2^* a_1^*)(b_3^* s_4 - s_3 b_4^*) + (c_3^* a_1^* - c_1^* a_3^*)(b_2^* s_4 - s_2 b_4^*)\\
&\quad + (c_1^* a_4^* - c_4^* a_1^*)(b_2^* s_3 - s_2 b_3^*) + (c_2^* a_3^* - c_3^* a_2^*)(b_1^* s_4 - s_1 b_4^*)\\
&\quad + (c_4^* a_2^* - c_2^* a_4^*)(b_1^* s_3 - s_1 b_3^*) + (c_3^* a_4^* - c_3^* a_4^*)(b_1^* s_2 - s_1 b_2^*),\\
\Delta_1 &= -\{\tilde{P}_1[a_2^*(b_3^* s_4 - b_4^* s_3) - a_3^*(b_2^* s_4 - b_4^* s_2) + a_4^*(b_2^* s_3 - b_3^* s_2)]\\
&\quad + \tilde{P}_2[c_2^*(b_3^* s_4 - s_3 b_4^*) - c_3^*(s_4 b_2^* - s_2 b_4^*) + c_4^*(s_3 b_2^* - s_2 b_3^*)]\}\tilde{\psi}(\xi, p),\\
\Delta_2 &= \{\tilde{P}_1[a_1^*(b_3^* s_4 - b_4^* s_3) - a_3^*(b_1^* s_4 - b_4^* s_1) + a_4^*(b_1^* s_3 - b_3^* s_1)]\\
&\quad - \tilde{P}_2[c_1^*(b_3^* s_4 - b_4^* s_3) - c_3^*(b_1^* s_4 - b_4^* s_1) + c_4^*(b_1^* s_3 - b_3^* s_1)]\}\tilde{\psi}(\xi, p),\\
\Delta_3 &= \{-\tilde{P}_1[a_1^*(b_2^* s_4 - b_4^* s_2) - a_2^*(b_1^* s_4 - b_4^* s_1) + a_4^*(b_1^* s_2 - b_2^* s_1)]\\
&\quad + \tilde{P}_2[c_1^*(b_2^* s_4 - s_2 b_4^*) - c_2^*(b_1^* s_4 - s_1 b_4^*) + c_4^*(b_1^* s_2 - s_1 b_2^*)]\}\tilde{\psi}(\xi, p),\\
\Delta_4 &= \tilde{P}_1[a_1^*(b_2^* s_3 - b_3^* s_2) - a_2^*(b_1^* s_3 - b_3^* s_1) + a_3^*(b_1^* s_2 - b_2^* s_1)]\\
&\quad + \tilde{P}_2[-c_1^*(s_3 b_2^* - s_2 b_3^*) + c_2^*(b_1^* s_3 - b_3^* s_1) - c_3^*(b_1^* s_2 - b_2^* s_2)]\}\tilde{\psi}(\xi, p).
\end{aligned} \tag{2.29}$$

2.3 Frequency domain solution

In this case we take time harmonic behaviour as

$$(u_1, u_2, \phi_3, T)(x_1, x_2, t) = (u_1, u_2, \phi_3, T)(x_1, x_2)\mathrm{e}^{i\omega t}. \tag{2.30}$$

In frequency domain, boundary condition at $x_2 = 0$ are given by

$$t_{22} = -P_1\psi(x_1)\mathrm{e}^{i\omega t}, \quad t_{21} = -P_2\psi(x_1)\mathrm{e}^{i\omega t}, \quad m_{23} = 0, \quad T = 0. \tag{2.31}$$

The expressions for normal stress, tangential stress, tangential couple stress and temperature distribution for concentrated and uniformly distributed forces in frequency domain can be obtained by replacing p by $i\omega$ in equations (2.28) and (2.29) and $\bar{\eta}(p)$ with $\mathrm{e}^{i\omega t}$. The solution due to an impulsive harmonic force moving along the positive x_1 axis with the uniform nondimensional velocity V at $x_2 = 0$ can be obtained by replacing $\psi(x_1, t)$ with $\delta(x_1 - Vt)$, whose Fourier transform with respect to x_1 is $\mathrm{e}^{i\xi Vt}$.

2.4 Steady state solution

Consider that the load is moving with a constant nondimensional velocity U in the negative x_1 direction then steady state is assumed to prevail in the neighborhood of the load as seen by an observer moving with the same speed in the same direction as that of the load. Following Fung [20], we introduce the Galilean transformation, i.e., $x_1^* = x_1 + Ut$, $x_2^* = x_2$, $t^* = t$, in the nondimensional equations, so that $\psi(x_1, t)$ in (2.14) will take the form of $\psi(x_1^*)$ defined by

$$\psi(x_1^*) = \begin{cases} \delta(x_1^*), \text{ for concentrated force} \\ H(x_1^* + a) - H(x_1^* - a), \text{ for uniformly distributed force.} \end{cases} \tag{2.32}$$

Applying (2.13) on the boundary conditions (2.14) where $\psi(x_1, t)$ is replaced by (2.32), and following the same procedure as in the case of time domain, we can obtain the expressions for normal stress, tangential stress, tangential couple stress and temperature distribution in steady state by replacing p with $-\mathrm{i}\xi U$ in (2.28) and (2.29), when concentrated and uniformly distributed forces are applied.

2.5 Inclined load

For an inclined load F_0, per unit length, we have

$$P_1 = F_0 \cos\theta, \quad P_2 = F_0 \sin\theta. \tag{2.33}$$

Using equation (2.33) in equations (2.28)-(2.29), we obtain the corresponding expressions for displacement and stress components in case of inclined load applied on the surface of half space.

3 Inversion of the Transformation

The transformed stresses and temperature distribution are functions of y, the parameters of Laplace and Fourier transforms p and ξ, respectively, and hence are of the form $\tilde{f}(\xi, x_2, p)$. To obtain the solution of the problem in the physical domain, we must invert the transform in (2.28) using

$$\bar{f}(x_1, x_2, p) = \frac{1}{2\Pi} \int_{-\infty}^{\infty} \tilde{f}(\xi, x_2, p) e^{-i\xi x_1} d\xi,$$

$$\bar{f}(x_1, x_2, p) = \frac{1}{2\Pi} \int_{-\infty}^{\infty} [\tilde{f}_e \cos(\xi x_1) - i \sin(\xi x_1) \tilde{f}_0] d\xi, \tag{3.1}$$

where f_e and f_0 are respectively even and odd parts of the function $\tilde{f}(\xi, x_2, p)$. Thus, expressions (3.1) give us the transform $\bar{f}(\xi, x_2, p)$ of the function $f(x_1, x_2, t)$. Now, for the fixed values of ξ, x_1 and x_2, the $\bar{f}(x_1, x_2, p)$ in the expression (3.1) can be considered as

the Laplace transformed function $\bar{g}(p)$ of some function g(t). Following Honig and Hirdes [21], the Laplace transformed function $\bar{g}(p)$ can be converted as given below.

The function $g(t)$ can be obtained by using

$$g(t) = \frac{1}{2\pi i} \int_{c-i\infty}^{c+i\infty} e^{pt} \bar{g}(p) dp, \tag{3.2}$$

where c is an arbitrary real number greater than all the real parts of the singularities of $\bar{g}(p)$. Taking $p = c + ix_2$, we get

$$g(t) = \frac{e^{ct}}{2\pi i} \int_{-\infty}^{\infty} e^{ity} \bar{g}(c + ix_2) dx_2. \tag{3.3}$$

Now, taking $e^{-ct}g(t)$ as $h(t)$ and expanding it as Fourier series in $[0, 2L]$, we obtain approximately the formula

$$g(t) = g_\infty(t) + E'_D,$$

where

$$g_\infty(t) = \frac{c_0}{2} + \sum_{k=1}^{\infty} c_k, \ 0 \le t \le 2L, \quad c_k = \frac{e^{ct}}{L} \Re\Big[e^{ik\pi t/L} \bar{g}\Big(c + \frac{ik\pi}{L}\Big)\Big]. \tag{3.4}$$

E_D is the discretization error and can be made arbitrarily small by choosing c large enough. The value of c and L are chosen according to the criteria outlined by Honig and Hirdes [21].

Since the infinite series in equation (3.4) can be summed up only to a finite number of N terms, the approximate value of $g(t)$ becomes

$$g_N(t) = \frac{c_0}{2} + \sum_{k=1}^{N} c_k, \ 0 \le t \le 2L. \tag{3.5}$$

Now, we introduce a truncation error E_T that must be added to the discretization error to produce the total approximation error in evaluating $g(t)$ using the above formula. Two methods are used to reduce total error. The discretization error is reduced by using the 'Korrecktur' method, Honig and Hirdes [21] and then 'ϵ-algorithm' is used the truncation error and hence to accelerate the convergence.

The 'Korrecktur' method formula, for evaluating the function $g(t)$, is

$$g(t) = g_\infty(t) - e^{-2cL} g_\infty(2L + t) + E_{D'},$$

where $|E'_D| \ll |E_D|$. Thus, the approximate value of $g(t)$ becomes

$$g_{N_k}(t) = g_N(t) - e^{-2cL} g_{N'}(2L + t), \tag{3.6}$$

where N' is an integer such that $N' < N$.

We shall now describe the $\epsilon-$algorithm which is used to accelerate the convergence of the series in equation (3.5). Let N be a natural number and $S_m = \sum_{k=1}^{m} c_k$ be the sequence of partial sums of equation (3.5). We define the ϵ-sequence by

$$\epsilon_{0,m} = 0, \qquad \epsilon_{1,m} = S_m,$$

$$\epsilon_{n+1,m} = \epsilon_{n-1,m+1} + \frac{1}{\epsilon_{n,m+1} - \epsilon_{n,m}}, \ n, m = 1, 2, 3 \ldots$$

It can be shown by Honig and Hirdes [10] that the sequence $\epsilon_{1,1}, \epsilon_{3,1}, \ldots, \epsilon_{N,1}$ converges to $g(t) + E_D - c_0/2$ faster than the sequence of partial $S_m, m = 1, 2, 3, \ldots$ The actual procedure to invert the Laplace Transform reduces to the study of equation (3.6) together with ϵ-algorithm.

The last step in the inversion process is to evaluate the integral (3.1). This has been done using Romberg's integration with adaptive size. This method uses the results from successive refinements of the extended trapezoidal rule followed by extrapolation of the results to the limit when the step size tends to zero. The details can be found in [22].

4 Numerical Results and Discussion

For numerical computations, we take the following nondimensional values for orthotropic micropolar thermoelastic solid:

$$d_1 = 1.02, \ d_2 = 0.7888, \ d_3 = 1.9828, \ d_4 = 6.0224,$$

$$d_5 = 1.32, \ d_6 = 1.53, \ d_7 = .00104, \ d_8 = 1.6543.$$

Following Gauthier [23] we take the following nondimensional values for aluminium epoxy like composite:

$$d_1 = 1, \ d_2 = 0.667, \ d_3 = .992, \ d_4 = 5.977,$$

$$d_5 = 1, \ d_6 = 1, \ d_7 = .001167, \ d_8 = .847.$$

Graphical representation of normal stress, tangential couple stress and temperature distribution for orthotropic micropolar generalized thermoelastic solid have been shown in Figures 1-9, to show the comparison between three different cases, viz., time domain (TD), frequency domain (FD) and steady state (SS). The computations were carried out at $x_2 = 0.1$ over the interval $(0, 10)$. The curves represented by solid lines with or without centre symbol correspond to the case of orthotropic micropolar generalized thermoelastic solid in time domain (TD), curves represented by dotted lines with or without centre symbol correspond to the case of orthotropic micropolar generalized thermoelastic solid in frequency domain (FD) and curves represented by large dashes lines with or without centre symbol correspond to the case of orthotropic micropolar generalized thermoelastic solid in steady state

(SS). All the results are presented for one value of nondimensional width $a = 1$ and for four values of nondimensional speed $V = 10, 20, 30, 40$. In Figures 1-6, curves without center symbol represent the variations corresponding to $\theta = 0$ (initial angle), while the curves with center symbol $(- \circ -)$ represent the variations for $\theta = 45$ (intermediate angle) and curves with center symbol $(- \times -)$ represent the variations for $\theta = 90$ (extreme angle). In Figures 7-9, curve without center symbol represent the variations for nondimensional speed $V = 10$, whereas curve with center symbol $(- \circ -), (-\Delta -), (- \times -)$ represent the variations corresponding to nondimensional speed $V = 20, 30, 40$, respectively.

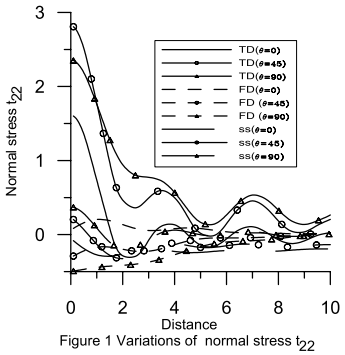

Figure 1 Variations of normal stress t_{22} due to concentrated force

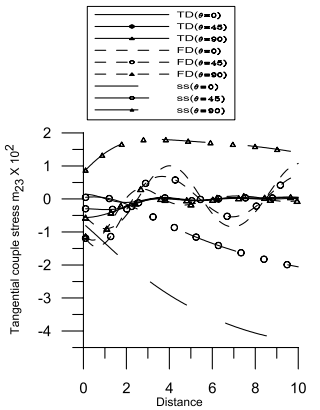

Figure 2 Variations of tangential couple stress m_{23} due to concentrated force

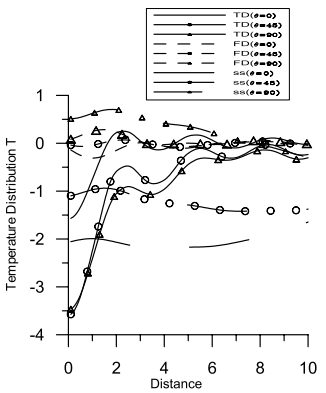

Figure 3 Variations of Temperature Distribution T due to concentrated force

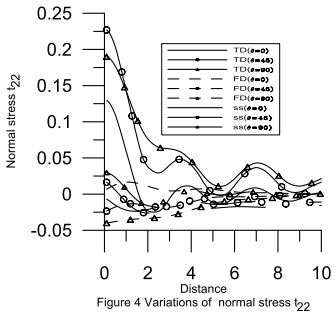

Figure 4 Variations of normal stress t_{22} due to distributed force

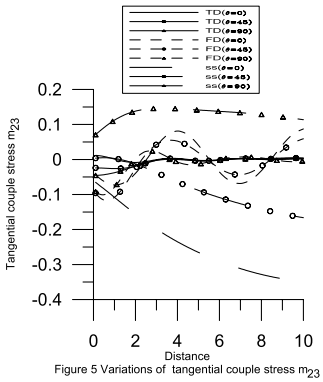

Figure 5 Variations of tangential couple stress m_{23} due to distributed force

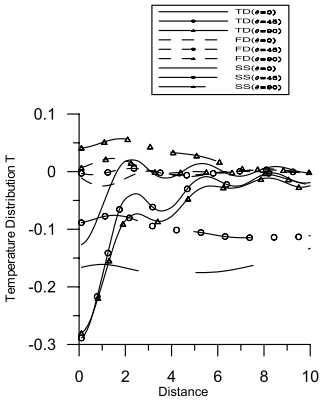

Figure 6 Variation of Temperature Distribution T due to distributed force

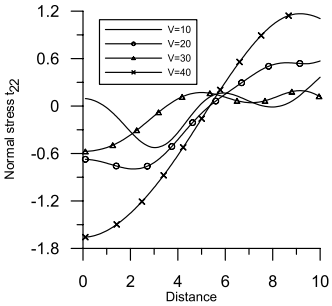

Figure 7 Variations of normal stress t_{22} due to moving force

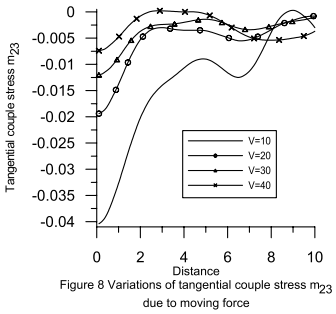

Figure 8 Variations of tangential couple stress m_{23} due to moving force

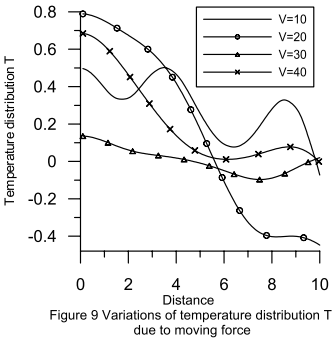

Figure 9 Variations of temperature distribution T due to moving force

4.1 Concentrated force

Figures 1-3 depict the variations of normal stress t_{22}, tangential couple stress m_{23} and temperature distribution T due to concentrated force.

Figure 1 shows the variation of normal stress t_{22} with distance in time domain, frequency domain and steady state. In time domain and at all angles of inclination, the value of normal stress t_{22} decreases sharply within the range $0 \leq x_1 \leq 2.5$, and then oscillate with further increase in distance. Its value in frequency domain and at initial and intermediate angle of inclination, initially increases then oscillate with very small amplitude, whereas at extreme inclination angle its value increases with increase in distance. However, in the case of steady state, the values of t_{22} follows an oscillatory pattern about zero value for all the values of θ.

It is evident from Figure 2 that in time domain and at $\theta = 0$ the value of tangential couple stress m_{23} initially decreases and then oscillate with very small amplitude, while its behaviour get reversed with increase in angle of inclination. In frequency domain and for all values of θ its value oscillates with large amplitude. However, the value of m_{23}, in the case of steady state, decreases with increase in distance when $\theta = 0, 45$ and initially increases and then decreases slowly with distance at extreme angle of inclination ($\theta = 90$). Figure 3 illustrates the variation of temperature distribution T with distance. The value of T in time domain and for at all angle of inclination i.e $\theta = 0, 45, 90$ increases sharply over the interval $(0, 2.5)$ and then oscillate with increasing amplitude. In frequency domain and at $\theta = 0, 45$, its value initially decreases, then increases and then oscillate with increase in distance. For the case of steady state and at initial and intermediate angle of inclination its value oscillates with small amplitude, while at extreme inclination, its value initially increases and then decreases with increase in distance.

4.2 Distributed force

Figures 4-6 show the variations of normal stress t_{22}, tangential couple stress m_{23} and temperature distribution T with distance in time domain, frequency domain and steady state when distributed force is applied. It is noticed from these figures that the variation pattern of t_{22}, m_{23}, T almost same to the pattern as observed in the case of concentrated force with difference in their amplitude of oscillation.

4.3 Moving force

Figures 7-9 show the variations of normal stress t_{22}, tangential couple stress m_{23} and temperature distribution T with distance x due to moving force.

It is depicted from Figure 7 that when $V = 10, 30$ the value of t_{22} initially decreases, then increases with increase in distance, whereas for $V = 20, 40$ its value get increased

with increase in distance. Figure 8 illustrates the variation of m_{23} with distance. At initial velocity its value increases within the range $0 \leq x_1 \leq 5, 7 \leq x_1 \leq 9$, decreases for remaining value of x_1. However, with further increase in velocity, its value oscillates with increase in distance. It is evident from Figure 7 that the maximum (absolute) tangential couple stress m_{23} occur corresponding to the maximum velocity ($V = 40$), i.e., impact of moving force is large for large velocities. Figure 9 shows the variation of temperature distribution T with distance. At initial velocity its value oscillates with decreasing amplitude. However, with further increase in V its value initially decreases and then oscillate with x.

5 Conclusion

It is observed from above discussion that the variation of temperature distribution is opposite to the variations obtained for normal stress in all the cases i.e. in time domain, frequency domain and steady state. With increase in the angle of inclination, the value of normal stress increases in amplitude in the case of time and frequency domain, while the reverse behaviour is observed in the case of steady state. Also, the value of temperature distribution in the cases of frequency domain and steady state increases with the increase in angle of inclination, while its value shows the opposite behaviour in the time domain. It is also depicted that the amplitude of the value of tangential couple stress increases with increase in angle of inclination for the case of steady state, while decreases with increase in θ in time domain. However, on the application of moving force, the value of tangential couple stress get increased with increase in velocity, while oscillatory pattern is depicted in the values of normal stress and temperature distribution.

References

[1] A. C. Eringen, Linear theory of Micropolar Elasticity, *J. Math. Mech.* **15** (1966), 909–923.

[2] A. C. Eringen, Theory of Micropolar Elasticity, in: Fracture, H. Liebowitz (ed.), Vol. II, Academic Press, New York, 1968.

[3] A. C. Eringen, Foundations of Micropolar Thermoelasticity, Course of Lectures No. 23, CSIM Udine Springer, 1970.

[4] D. Iesan, Some applications of micropolar mechanics to earthquake problems, *Internat. J. Engrg. Sci.* **19** (1981), 855–864.

[5] W. Nowacki, Couple Stress in the Theory of Thermoelasticity, Proc. ITUAM Symposia, Vienna, Editors H. Parkus and L. I. Sedov, Springer-Verlag, 1966, pp, 259–278.

[6] A. C. Eringen, Balance laws of micromorphic continua. *Internat. J. Engrg. Sci.* **30** (1992), 805–810.

[7] T. R. Tauchert, W. D. Claus, and T. Ariman, The linear theory of micropolar thermoelasticity, *Internat. J. Engrg. Sci.* **6** (1968), 637–47.

[8] S. Dost and B. Tabarrak, Generalised micropolar thermoelasticity. *Internat. J. Engrg. Sci.*, **16** (1978), 173–183.

[9] R. S. Dhaliwal and A. Singh, Micropolar Thermoelasticity, in: Thermal stresses II, mechanical and mathematical methods, Ser.2, R. Hetnarski (Ed.), North-Holland, 1987.

[10] D. S. Chandershekharia, Heat flux dependent micropolar thermoelasticity. *Internat. J. Engrg. Sci.* **24** (1986), 1389–1395.

[11] D. Iesan, On the positive definiteness of the operator of micropolar elasticity, *J. Engrg. Math.* **8** (1974), 107–112.

[12] R. Kumar and P. Aliwalia, Elastodynamics of inclined loads in a micropolar cubic crystal, *Mech. and Mechanical Engg.* **9** (2005), 57–75.

[13] R. Kumar and P. Aliwalia, Moving inclined load at boundary surface, *Appl. Math. Mech. (English Ed.)* **26** (2005), 476–485.

[14] R. Kumar and P. Aliwalia, Interactions due to inclined load at micropolar elastic half-space with voids, *Int. J. Appl. Mec. and Engg.* **10** (2005), 109–122.

[15] R. Kumar and L. Rani, Response of thermoelastic half-space with voids due to inclined load, *Int. J. Appl. Mec. and Engg.* **10** (2005), 281–294.

[16] R. Kumar and L. Rani, Deformation due to inclined load in thermoelastic half space with voids, *Arch. Mech.*, **57** (2005), 7–24.

[17] R. Kumar and S. Choudhary, Response of orthotropic micropolar medium under the influence of various sources, *Mechanica*, **38** (2003), 349–368.

[18] R.Kumar and S. Choudhary, Dynamical behaviour of orthotropic micropolar elastic medium, *J. Vibration. Control*, **8** (2004), 1053–1069.

[19] R. Kumar and P. Ailawalia, Effects of fluid layer at micropolar orthotropic boundary surface, *Sādhanā*, **29** (2004), 605–616.

[20] Y. C. Fung, Foundations of Solid Mechanics, Prentice Hall, New Delhi, 1968.

[21] G. Honig and V. Hirdes, A method for the numerical inversion of the Laplace transform, *J. Comput. Appl. Math.* **10** (1984), 113–132.

[22] W. H. Press, S. A.Teukolshy, W. T. Vellering, and B. P. Flannery, Numerical Recepies, Cambridge University Press, Cambridge, 1986.

[23] R. D. Gauthier, In Experimental investigations on micropolar media, Mechanics of micropolar media, O. Brulin and RKT Hsieh (eds), World Scientific, Singapore, 1982.

Rajneesh Kumar was born on 08-08-1958. He earned a M.Sc. (1980) from Guru Nanak Dev University (G.N.D.U.), Amritsar (Punjab), a M.Phil. (1982) from Kurukshetra University Kurukshetra (K.U.K.) and a Ph.D. (1986) in Applied Mathematics from Guru Nanak Dev University (G.N.D.U.), Amritsar. He guided 52 M.Phil. students, 9 Ph.D. students

and currently, he is supervising 8 Ph.D. students. He has published 181 papers various international journals. His area of research work is Continuum Mechanics (Micropolar elasticity, thermoelasticity, poroelasticity, magnetoelasticity, micropolar porous couple stress theory, viscoelasticity, mechanics of fluid.)

Rajani Rani Gupta earned her B. Sc. and M. Sc. in Mathematics from University of Pune, India in 2003 and 2005, respectively. Presently she is pursuing a Ph.D. at Kurukshetra University, India. She has 4 published papers and 7 accepted papers in several international journals.